The Astrophysical Journal, 624:923–933, 2005 May 10

MV LYRAE IN LOW, INTERMEDIATE, AND HIGH STATES[1]

Albert P. Linnell,[2] Paula Szkody,[3] Boris Gänsicke,[4] Knox S. Long,[5] Edward M. Sion,[6]
D. W. Hoard,[7] and Ivan Hubeny[8]
Received 2004 November 5; accepted 2005 January 24

ABSTRACT

Archival *IUE* spectra of the VY Sculptoris system MV Lyrae, taken during an intermediate state, can be best fit by an isothermal accretion disk extending half-way to the tidal cutoff radius. In contrast, a recent *HST* spectrum, while MV Lyr was in a high state, can be best fit with a standard $T(R)$ profile for an accretion disk extending from an inner truncation radius to an intermediate radius with an isothermal accretion disk beyond. These fits use component-star parameters determined from a study of MV Lyr in a low state. Model systems containing accretion disks with standard $T(R)$ profiles have continua that are too blue. The observed high-state absorption-line spectrum exhibits excitation higher than provided by the $T(R)$ profile, indicating likely line formation in a high-temperature region extending vertically above the accretion disk. The absorption lines show a blueshift and line broadening corresponding to formation in a low-velocity wind apparently coextensive with the high-temperature region. Lines of N v, Si iv, C iv, and He ii are anomalously strong relative to our synthetic spectra, indicating possible composition effects, but unmodeled excitation effects could also produce the anomalies. An analysis of a low state of MV Lyr, considered in an earlier study and extended in this paper, sets a limit of 2500 K for the $T_{\rm eff}$ of an accretion disk that may be present in the low state. This limit is in conflict with two recent models of the VY Sculptoris phenomenon.

Subject headings: accretion, accretion disks — novae, cataclysmic variables — stars: individual (MV Lyrae) — ultraviolet: stars — white dwarfs

Online material: color figures

1. INTRODUCTION

Cataclysmic variables (CVs) are binary stars consisting of a white dwarf (WD) and a late spectral type secondary that fills, or almost fills, its Roche lobe and transfers mass to the WD. CVs divide into a number of subclasses (Warner 1995), and the object of our study, MV Lyrae, is a novalike CV of the VY Sculptoris subclass. A defining characteristic of this subclass is a nonperiodic alternation between high and low luminosity states, differentiated by a change in mean brightness of more than 1 mag between states. This alternation usually takes place on intervals of hundreds of days.

The orbital period of MV Lyr, 3.19 hr, places it close to the long-period end of the period gap (Warner 1995). Its high-low range is 12.2–18, inferred from Figure 4 of Honeycutt & Kafka (2004). While it is widely argued that evolution of CVs with periods longer than the period gap is controlled by magnetic braking (Patterson 1984; King 1988) and that evolution shortward of the gap is driven by gravitational radiation (King 1988), this scenario has been recently challenged by, e.g., Andronov et al. (2003), King & Schenker (2002), and Schenker & King (2002). Patterson (1984) developed an empirical mass transfer relationship for CVs that predicts a mass transfer rate of $2.5\times10^{-10}\ M_\odot\ {\rm yr}^{-1}$ at the orbital period of MV Lyr. A theory of magnetic braking (Hameury et al. 1988) shows that the mass transfer rate from the secondary is a decreasing function with decreasing orbital period, reaching a value of $1.0\times10^{-9}\ M_\odot\ {\rm yr}^{-1}$ at the top of the period gap, where MV Lyr is found, for the parameters used in their study. Some authors, as discussed below, adopt even larger mass transfer rates at the top of the period gap.

If the magnetic braking mechanism that drives evolution of the secondary star is suddenly turned off at an orbital period of 3 hr, then the secondary approaches thermal equilibrium on a Kelvin-Helmholtz timescale. Consequently, mass transfer continues at a decreasing rate for $\approx10^4$ yr (Ritter 1988). But the alternation between high and low states in VY Sculptoris stars is on a much shorter timescale and requires a separate mechanism to switch the mass transfer on and off. Livio & Pringle (1994) discuss the problem and propose starspots on the secondary star that pass across the L1 point and cause reduced mass transfer. This proposal has been further developed (King & Cannizzo 1998) with application of a time-dependent code to model the variable accretion disk (see also Schreiber et al. 2000). But the King & Cannizzo (1998) model produced the unwanted result of dwarf nova type outbursts in the low state, after mass transfer had been switched off. A suggested escape was maintenance of the inner accretion disk in a permanent high state through irradiation by the WD (Leach et al. 1999, hereafter L99). L99 concluded that the presence of a 40,000 K WD does suppress dwarf nova outbursts. The L99 study adopted a high-state mass transfer rate

[1] Based on observations made with the NASA/ESA *Hubble Space Telescope*, obtained at the Space Telescope Science Institute, which is operated by the Association of Universities for Research in Astronomy, Inc., under NASA contract NAS5-26555, and with the Apache Point Observatory 3.5 m telescope, which is operated by the Astrophysical Research Corporation.

[2] Department of Astronomy, University of Washington, Box 351580, Seattle, WA 98195-1580; linnell@astro.washington.edu.

[3] Department of Astronomy, University of Washington, Box 351580, Seattle, WA 98195-1580; szkody@astro.washington.edu.

[4] Department of Physics, University of Warwick, CV4 7AL, Coventry, UK; boris.gaensicke@warwick.ac.uk.

[5] Space Telescope Science Institute, 3700 San Martin Drive, Baltimore, MD 21218; long@stsci.edu.

[6] Department of Astronomy and Astrophysics, Villanova University, Villanova, PA 19085; edward.sion@villanova.edu.

[7] *Spitzer* Science Center, California Institute of Technology, Mail Code 220-6, 1200 East California Boulevard, Pasadena, CA 91125; hoard@ipac.caltech.edu.

[8] NOAO, 950 North Cherry Avenue, Tucson, AZ 85726; and Steward Observatory and Department of Astronomy, University of Arizona, Tucson, AZ 85721; hubeny@noao.edu, hubeny@as.arizona.edu.

of $1.1\times10^{-8}\ M_{\odot}\ \mathrm{yr}^{-1}$ that was chosen to guarantee that hydrogen is fully ionized at the outer accretion disk boundary. According to L99, cessation of mass transfer produces a rapid transition to a state of low but nonzero viscosity. The accretion disk remains nearly intact during the low state, transferring only a few percent of the accretion disk mass to the WD. Because of nonzero viscosity, the accretion disk still radiates at a low level during the low state. Hameury & Lasota (2002, hereafter HL02) show that the adopted WD mass in L99 ($0.4\ M_{\odot}$) is important to the suppression of outbursts, and that a WD mass of $0.7\ M_{\odot}$ would have produced outbursts. HL02 alternatively propose that VY Sculptoris stars have magnetic WDs and that the magnetic field truncates the accretion disk. HL02 show that, for a WD mass of $0.7\ M_{\odot}$ and a magnetic moment of $\mu = 5\times10^{30}$ G cm^3, no outbursts occur and the change in the V magnitude, from high state to low state, is 5 mag.

Hoard et al. (2004, hereafter H04) used the BINSYN suite (Linnell & Hubeny 1996) to calculate a system model and corresponding synthetic spectrum for MV Lyr in a recent low state. The synthetic spectrum accurately fits *FUSE* spectra and contemporaneous optical spectra, as well as *IUE* spectra from a prior low state. The H04 discussion considers the connection of the low-state study to earlier investigations of MV Lyr and shows that the low state can be understood in terms of a naked hot WD with a temperature of 47,000 K, a photosphere log g of 8.25, and a metallicity of 0.3 solar. The log g, together with the mass-radius relation for zero-temperature carbon WD models (Hamada & Salpeter 1961), selects a model with $M_{\rm wd} = 0.73\ M_{\odot}$, estimated error of $0.1\ M_{\odot}$, and radius of $0.01067\ R_{\odot}$. The secondary star fills its Roche lobe and is cooler than 3500 K; it contributes nothing to the FUV flux and a varying amount to the optical flux, from 10% at 5200 Å to 60% at 7800 Å. If an accretion disk is present it contributes negligibly to the observed spectra. Assuming that no disk is present, the model optical light curve, for a system orbital inclination of 12° taken from the literature, has an amplitude approximately 50% larger that of the observed optical light curve. The scaling of the model spectrum to the observed data leads to a distance of $d = 505 \pm 50$ pc to MV Lyr.

In § 2 of this paper we describe the program suite used to analyze the observed spectra. In § 3 we further investigate the low state and derive improved system parameters. In § 4 we show that it is possible to augment the low-state system with an accretion disk with artificially elevated $T_{\rm eff}$ at large radii and achieve a close fit to intermediate-state *IUE* archival spectra. In § 5 we show that our models produce a predicted ΔV, low state to intermediate state, that is 1 mag larger than observed, indicating a problem with the models. In § 6 we show that an isothermal 14,000 K accretion disk extending half-way to the tidal cutoff radius resolves the ΔV problem and provides a fair fit to the *IUE* spectra. Section 7 presents a model fit to a new high-state *HST* spectrum, § 8 considers the predicted luminosity change low state to high state, a general discussion is in § 9, and § 10 summarizes our results.

2. DESCRIPTION OF THE BINSYN PROGRAM SUITE

The BINSYN suite (Linnell & Hubeny 1996), used in the analysis presented in this paper, is a set of programs for calculating synthetic spectra and synthetic light curves of binary star systems with or without accretion disks and in circular or eccentric orbits. The model stars have photospheres of assigned Roche potentials, defined by grids of points with associated photospheric segments. Program modules assign $T_{\rm eff}$ values to individual stellar points based on adopted polar $T_{\rm eff}$ values, bolometric albedos, and gravity-darkening exponents. Model stars may rotate synchronously or nonsynchronously up to critical rotation. Program modules calculate log g values at stellar photosphere points based on adopted Roche potentials and stellar masses, while other modules determine whether a given point is visible to the observer for a point on a star, the accretion disk face, or the accretion disk rim, and for the current values of orbital inclination and orbital longitude. Calculation of a synthetic spectrum uses a set of precalculated source synthetic spectra for each system object (stars, accretion disk face, accretion disk rim). The source spectra for a given object typically form a two-dimensional set in $T_{\rm eff}$ and log g that encompasses the extreme $T_{\rm eff}$ and log g values on the photosphere of the given object. Program modules interpolate an individual synthetic spectrum to each stellar photospheric point and integrate over that star, with allowance for point visibility; the routines properly allow for Doppler shift and line broadening.

TABLE 1
BINSYN Model System Parameters

Parameter	Value	Parameter	Value
$M_{\rm wd}$	$0.73\ M_{\odot}$	$r_{\rm wd}$	0.01017
q	0.43	log $g_{\rm wd}$	8.25
P	0.1329 days	r_s (pole)	0.28782
D	$1.11120\ R_{\odot}$	r_s (point)	0.40362
$\Omega_{\rm wd}$	98.74	r_s (side)	0.30011
Ω_s	2.74	r_s (back)	0.33258
i	7°0	log g_s (pole)	4.95
$T_{\rm eff,wd}$	47000 K	log g_s (point)	3.61
$T_{{\rm eff},s}$ (pole)	2600 K	log g_s (side)	4.87
$A_{\rm wd}$	1.0	log g_s (back)	4.68
A_s	0.5	r_a	$0.47\ R_{\odot}$
$b_{\rm wd}$	0.25	r_b	$0.01\ R_{\odot}$
b_s	0.08	H	$0.0110\ R_{\odot}$

Notes.—Subscript "wd" refers to the WD; subscript s refers to the secondary star. D is the component separation of centers, Ω is a Roche potential. Temperatures are polar values, A values are bolometric albedos, and b values are gravity-darkening exponents. Note that $r_{\rm wd}$ and the r_s values are in units of component separation, not solar radii. The quantity r_a specifies the outer radius of the accretion disk, set at the tidal cutoff radius, and r_b is the accretion disk inner radius, while H is the semiheight of the accretion disk rim.

An accretion disk is specified in BINSYN by an inner and outer radius, and the accretion disk is divided into a specified number of cylindrical annuli, with each annulus divided into a specified number of segments. Radiation characteristics of the accretion disk depend on a temperature profile, $T(R)$, of the accretion disk annuli. We reserve the term "standard model" to designate a $T(R)$ relation

$$T(R) = W\left\{\frac{3GM\dot{M}}{8\pi R_*^3\sigma}\left[1-\left(\frac{R_*}{R}\right)^{1/2}\right]\right\}^{1/4}\left(\frac{R}{R_*}\right)^{\beta}, \quad (1)$$

with $\beta = -0.75$ for the standard model (Frank et al. 1992, p. 78). Here W is a normalizing factor (not a dilution factor); $W = 1.0$ for the standard model. For default conditions, our definition is algebraically identical to the Frank et al. definition.

The accretion disk is flared, in the sense that successive annuli step up in height between the inner radius and a specified semiheight at the outer radius. Let H be the semithickness at the outer radius r_a, and let r_b be the inner radius. Then the semithickness at radius r, $h(r)$, is $h(r)/H = (r - r_b)/(r_a - r_b)$ (see Table 1). In calculating a model for an accretion disk system, BINSYN by default assigns $T_{\rm eff}$ values to annuli based on the standard model, appropriate to an assumed mass transfer rate. An option permits modification of the assigned annulus $T_{\rm eff}$ values to include calculated irradiation by the WD, based on a bolometric albedo formalism. Calculation of a synthetic spectrum for the accretion disk, as part of the calculation of the system synthetic spectrum, involves interpolation among previously calculated source spectra (with their individual $T_{\rm eff}$ values) to produce a synthetic spectrum for each annulus, for its $T_{\rm eff}$ as assigned by BINSYN. The accretion disk source spectra may consist largely of synthetic spectra for annulus models produced by TLUSTY (Hubeny 1988; Hubeny & Lanz 1995). This calculation is followed by integration over all annuli, with detailed allowance for Doppler shifts and sources of line broadening and with proper allowance for visibility to the observer. The number of source spectra typically will differ from the specified number of annuli. The programs finally output the calculated flux as function of wavelength for the individual objects as well as their sum, which represents the system synthetic spectrum at the current orbital longitude. A parallel procedure produces synthetic light values, repeated for a grid of orbital longitudes, and so leads to light curves for specified wavelengths. Additional details are in Linnell & Hubeny (1996).

3. FIT TO THE LOW-STATE OPTICAL SPECTRA

In fitting the optical spectra, H04 found two difficulties: (1) The polar $T_{\rm eff}$ of the secondary was cooler than 3500 K, which is the temperature of the coolest (Kurucz) model atmosphere available to us. (2) The optical spectra were observed through thin clouds, so an empirical scaling factor was applied to the observed fluxes to match them to the synthetic spectrum (the latter was scaled to fit the FUV spectrum).

Figure 8 of H04 shows the model fit to observed spectra, covering the interval 930–7800 Å, including archived *IUE* spectra SWP10905 covering 1150–1978 Å and LWR09590 covering 1851–3349 Å, which were obtained on 1980 December 27. Figure 1 of this paper presents the model fit to the same low-state *IUE* spectra in much greater detail than in H04. Note that Figure 8 of H04 is a logarithmic plot while Figure 1 of this paper plots flux directly. In producing Figure 1, the spectra were divided by the same scaling factors applied in the H04 plots (2.43×10^{29} for the WD synthetic spectrum, 1.0×10^{-13} for the *IUE* spectra), set by the fit to the *FUSE* spectrum. The mean residual of the fit to the 877 points between 1150 and 3000 Å was 0.012, and the mean

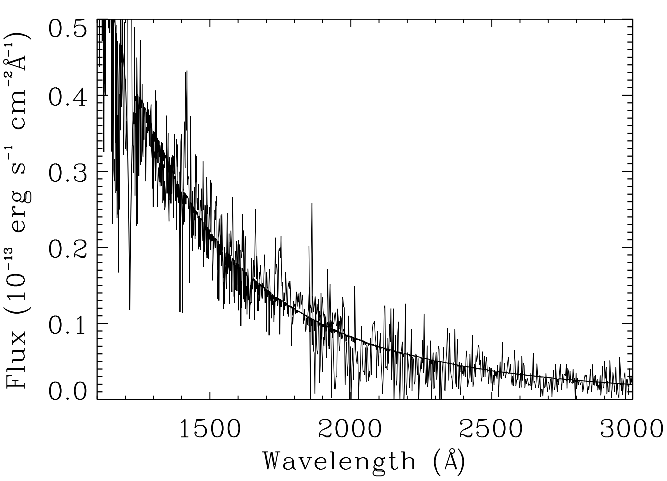

FIG. 1.—Fit of synthetic WD spectrum to low-state *IUE* spectrum of MV Lyr. The light line is the *IUE* spectrum; the heavy line is the synthetic spectrum. [*See the electronic edition of the Journal for a color version of this figure.*]

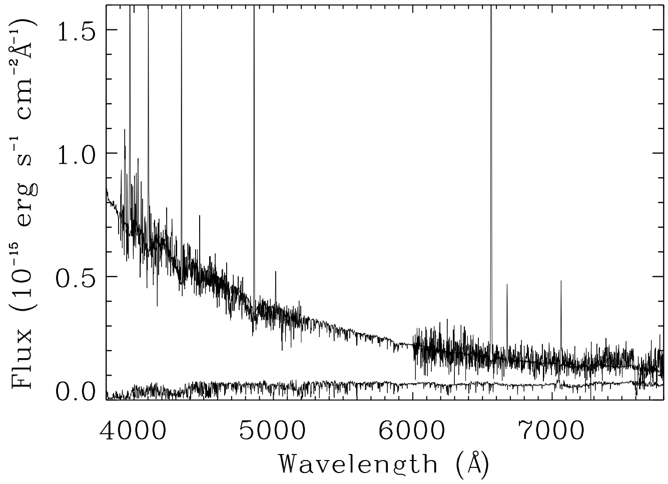

FIG. 2.—Fit of synthetic spectrum to low-state optical spectra of MV Lyr. The light line indicates the optical spectra; the heavy line is the system synthetic spectrum. The secondary-star contribution to the system synthetic spectrum is the lower spectrum in the plot. [*See the electronic edition of the Journal for a color version of this figure.*]

absolute residual was 0.038. These residuals apply to the scaled spectra. An important conclusion from the Figure 1 fit is that there is no evidence for the presence of an accretion disk. In a test of the sensitivity of the fit to added flux from a putative accretion disk, we find empirically that the addition of 0.005 flux units (Fig. 1 ordinates) produces a visually detectable displacement of the summed spectrum from the Figure 1 fit. At 3000 Å, the secondary star makes a calculated contribution of 0.1% to the system flux.

H04 fit an optical (unfiltered) light curve of MV Lyr (their Fig. 7). This fit was derived from the BINSYN spectral model described above. It assumes an orbital inclination for the CV of $i = 12^\circ$ from Skillman et al. (1995). However, the corresponding amplitude of the model light curve is 50% too large. The orbital period light variation results from the variable presentation of the irradiated secondary component to the observer. As the assumed inclination decreases from $i = 12^\circ$, the light amplitude decreases monotonically. An improved fit (Linnell et al. 2005) implies a system inclination of $i = 7^\circ \pm 1^\circ$, which we adopt for this analysis.

A remark is in order on the absolute accuracy of the results obtained in this paper. A key step is in the determination of the WD mass and radius in units of the solar values by comparison between the MV Lyr WD log g from our analysis of the *FUSE* spectrum and the log g values for the Hamada & Salpeter (1961) carbon WD models. The mass ratio q comes from relatively uncertain radial velocity measurements (Skillman et al. 1995), and this value determines the mass of the secondary star and, since the secondary fills its Roche lobe, the size of the secondary star. The fit of our synthetic spectra to FUV data, in all cases, applies a scaling divisor of 2.43×10^{29} to observed spectra, which were divided by 1.0×10^{-13} (see the ordinate labels). The scaling divisor may be inaccurate by 10%–15%.

We present here an improved representation of the secondary star using the NextGen synthetic spectra for M stars, version 5 (Hauschildt et al. 1999). We find a good fit to the observed spectra with a polar $T_{\rm eff} = 2600$ K. Irradiation by the 47,000 K WD produces a calculated L1 point $T_{\rm eff} = 5344$ K on the secondary star. BINSYN interpolated among seven NextGen synthetic spectra with $T_{\rm eff}$ values between 2600 and 5400 K to determine flux values for individual secondary-star photospheric segments. The fit of the system synthetic spectrum to the optical spectra is shown in Figure 2. The optical spectra were multiplied

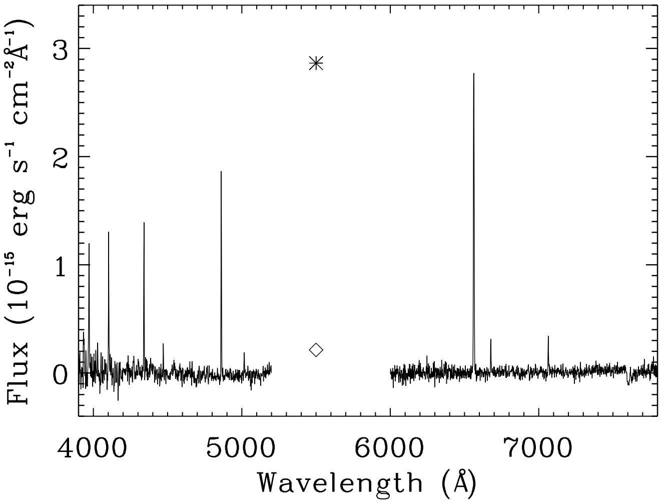

FIG. 3.—O (optical spectra) − C (synthetic spectrum) residual spectrum from Fig. 2. The asterisk marks the 5500 Å flux of the L99 model (see text) if it is placed at the distance of MV Lyr, while the diamond marks the corresponding datum for the HL02 model (see text). The feature at 7600 Å is due to the molecular oxygen "A" absorption band in the terrestrial atmosphere. The emission lines are produced on the secondary star by irradiation from the primary star.

by an empirically determined factor of 2 to correct for obscuration by clouds.

Recapitulating, we have developed a model for the low state of MV Lyr consisting of a 47,000 K WD and a secondary star with a polar $T_{\rm eff}$ of 2600 K. The secondary star fills its Roche lobe and is irradiated by the WD. The model has no accretion disk and differs from the model in H04 only in the improved representation of the secondary star in the calculated synthetic spectra. This model produces an excellent fit to the *FUSE* data, the low-state *IUE* data, and the optical data. We proceed to compare our model to the low-state predictions of L99 and HL02.

L99 (their Fig. 3) predict an accretion disk luminosity in the low state of $F_{5500} = 7.0 \times 10^{27}$ ergs s^{-1} Å^{-1}. Figure 3 plots the residual of the L99 accretion disk (*asterisk*) for the 505 pc (H04) distance of MV Lyr. The residual is F_{5500}/d^2, where $d = 505$ pc. The L99 accretion disk flux at 5500 Å would have to be approximately 60 times fainter to accord with the residual plot.

We calculated a synthetic spectrum for the example in HL02, with $\mu_{30} = 5$, with $M_{\rm wd} = 0.73\ M_\odot$ and mass ratio $q = 0.43$. The calculated inner radius for the HL02 example (their eq. [4]) is $r_{\rm in} = 5.7 \times 10^8$ cm and the MV Lyr WD radius is $r_{\rm wd} = 7.9 \times 10^8$ cm. Consequently, we set the inner accretion disk radius equal to the WD radius, the outer radius equal to the tidal truncation radius, and the mass transfer rate equal to $\dot{M} = 2 \times 10^{17}$ g s^{-1} (HL02 value). We used the synthetic spectrum of the calculated accretion disk alone in the following comparison. We divided the output flux in the synthetic spectrum by 100.0, the factor by which the HL02 model luminosity drops between the high and low states, to provide the HL02 model flux to compare with our low-state data. As with L99, this calculated low-state luminosity is a residual [(system model) − (BINSYN low-state model)], shown in Figure 3 by a diamond. It could be argued that division by 100.0 for all wavelengths is too simplistic in transforming the HL02 model to an equivalent low state, particularly since we have no observational data in the 5000–6000 Å interval. Our Figure 2 shows that the low-state synthetic spectrum varies smoothly over this wavelength interval, as do our intermediate-state model and high-state model, discussed in the following sections (not shown in separate figures). Thus, we believe the division by 100.0 is appropriate. The HL02 flux needs to be smaller by approximately a factor of 5–10 to agree with the spectral residuals. Thus, we find a discrepancy between the predictions of both L99 and HL02 for the MV Lyr low state and our fit to available low-state data.

How cool would an MV Lyr accretion disk have to be in the low state to avoid detection in optical spectra? Tests with an isothermal accretion disk, represented by a blackbody and truncated at $r = 1.7r_{\rm wd}$ (see the following text for a discussion of the truncation radius), demonstrate that an accretion disk must have a $T_{\rm eff}$ value of less than 2500 K to avoid a conflict with our optical spectra (a 2500 K accretion disk would provide a detectable 3% of the system flux at 7800 Å). A study of TT Ari (Gänsicke et al. 1999) obtained comparable results. A possible accretion disk would need to be truncated at $r = 12r_{\rm wd}$ and have a $T_{\rm eff}$ value of less than 3000 K to satisfy the low-state optical spectra.

4. FIT TO THE INTERMEDIATE-STATE *IUE* SPECTRA

The *IUE* archives include 10 spectra of MV Lyr. None of these were obtained during a high state, and two, SWP07296 and LWR06288, were obtained on 1979 December 2 during an intermediate state. Intermediate states are roughly 1 mag fainter than high states.

Figure 8 of H04 shows the intermediate-state *IUE* spectra on the same plot as the fit to the *FUSE*/*IUE*/optical low-state spectra, for comparison. A striking feature of the intermediate-state *IUE* spectra is their much lower (i.e., less blue) spectral gradient than the low-state *IUE* spectra. This is surely due to the presence of an optically thick accretion disk.

We calculated a series of annulus models using TLUSTY, version 200 (Hubeny 1988; Hubeny & Lanz 1995), for individual mass transfer rates of 1.0×10^{-9}, 4.0×10^{-9}, and $1.0 \times 10^{-8}\ M_\odot$ yr^{-1}. These latter models were spaced in values of $r/r_{\rm wd}$ between 2.5 and an outer value of $r/r_{\rm wd} = 28.5$, $T_{\rm eff} = 10{,}620$ K. TLUSTY includes a large number of optional control flags that control the program performance. We preserved the default control flags and thereby produced LTE thin-disk models with thin photospheres. Convergence problems intervened for larger values of $r/r_{\rm wd}$. We used a viscosity parameter $\alpha = 0.1$ (Shakura & Sunyaev 1973) for all models. The models included opacity contributions from the 30 most abundant periodic table elements. We used these models to calculate source (see above) synthetic spectra via SYNSPEC, version 48 (Hubeny et al. 1985), for all models, with the same opacities used for the model calculations. We included synthetic spectra for Kurucz stellar model atmospheres, calculated with SYNSPEC, to handle assigned temperatures cooler than the 10,897 K limit described above. Comparison among the annulus source synthetic spectra for the different tabular mass transfer rates showed that spectra for different mass transfer rates but similar $T_{\rm eff}$ values are essentially identical. Consequently, it is permissible to fix the source synthetic spectra of the annuli at some specific tabular mass transfer rate but change the BINSYN mass transfer rate for a new simulation and still produce a valid system synthetic spectrum.

The accuracy of the accretion disk synthetic spectrum is sensitive to the $T_{\rm eff}$ spacing of the source synthetic spectra. Linear interpolation between source spectra differing in $T_{\rm eff}$ values by several thousand kelvins can produce an inaccurate interpolated spectrum. After extensive experiment, we adopted a "universal" set of 69 source spectra, of which 62 were TLUSTY models. These latter models had $T_{\rm eff}$ values spaced at roughly 500 K intervals between 10,620 and 31,564 K and a slightly larger step between 31,564 and 63,735 K. The remaining synthetic spectra were for Kurucz models covering the $T_{\rm eff}$ range 5000–10,000 K. In the wavelength range of interest, contributions from ≈7000 K or cooler $T_{\rm eff}$ values are very small or negligible.

Our initial study of the intermediate state adopted a variety of assumed mass transfer rates, together with a standard model accretion disk. We used the system parameters of Table 1, and BINSYN in a diagnostic mode, to attempt a fit to the intermediate-state *IUE* spectra. With the exception of the parameters D, i, $T_{{\rm eff},s}$, r_a, r_b, and H (see Table 1 comments), the Table 1 parameters for the WD and secondary star are the same as in H04. Our model divides the accretion disk into 66 annuli, with each annulus divided into 90 azimuthal segments. The system synthetic spectrum is the integrated sum of the contributions of the WD, secondary component, accretion disk, and accretion disk rim. (Note that at an inclination of 7°, the accretion disk rim contributes a negligible observable effect.)

We find that it is not possible to fit the intermediate-state *IUE* spectra by adding a standard model accretion disk to the low-state model of H04 and using our TLUSTY annulus synthetic spectra. The radial temperature gradient in the standard model produces either too much flux at short wavelengths or too little flux at long wavelengths. In making this (and all subsequent) comparisons with the *IUE* spectra, we maintained the same scaling divisors for both the *IUE* spectra and the synthetic spectrum that were adopted for the low-state comparison. Given the measured $E(B-V)=0.0$ (Szkody & Downes 1982), we applied no interstellar extinction corrections to the *IUE* spectra extracted from the archive. Figure 4 illustrates the discrepancy produced by adding an accretion disk component with a mass transfer rate of $1.0\times10^{-9}\ M_\odot\ {\rm yr}^{-1}$. Note that this rate equals the value given by Hameury et al. (1988) at the top of the period gap. This mass transfer rate, and a standard model disk, produces disk $T_{\rm eff}$ values ranging from 23,765 K at the inner disk edge to 4222 K at the outer disk edge, with a temperature maximum of 34,972 K at $r=1.3611r_{\rm wd}$. The absolute flux from the accretion disk, at the Earth, is a strong function of the mass transfer rate, and the approximate fit in Figure 4 indicates that the adopted mass transfer rate is nearly correct; i.e., the *mean* residual over the wavelength interval plotted is small. The synthetic spectrum is too blue. A larger mass transfer rate increases the flux at all wavelengths, making the mean residual larger, and produces a synthetic spectrum that is too blue. A smaller mass transfer rate decreases the flux at all wavelengths, again making the mean residual larger, and produces a synthetic spectrum that is too blue.

The Figure 4 residuals suggest a departure from the standard model. Stationary models are possible (Lasota 2001) whose $T(R)$ profiles differ from the standard model. Examples include systems in which irradiation by the WD is important, or systems in which the mass transfer stream directly heats the outer regions of the accretion disk (Visniac & Diamond 1989, 1992; Smak 1994; but see Armitage & Livio 1998) or in which there is an increased mass flux through the outer part of the accretion disk for unspecified reasons (Křiž & Hubeny 1986). In all of our synthetic spectra, the synthetic spectrum has absorption lines where the *IUE* spectrum shows emission lines. Skillman et al. (1995) argue that the broad emission lines in the high ($V\sim$ 13–14) state arise from the accretion disk, in contrast to narrow (Fig. 2) emission lines produced on the irradiated secondary when MV Lyr is in a low state.

Two variations of the standard model $T(R)$ relation affect the corresponding system synthetic spectrum: (1) a change in the functional dependence of $T(R)$ on R (Orosz & Wade 2003) and (2) truncation of the accretion disk at some inner radius larger than the WD radius (Long et al. 1994). Physically, truncation can occur either by evaporation of the inner disk annuli (Hameury et al. 2000) or by accretion disk interaction with a magnetic field associated with the WD (HL02).

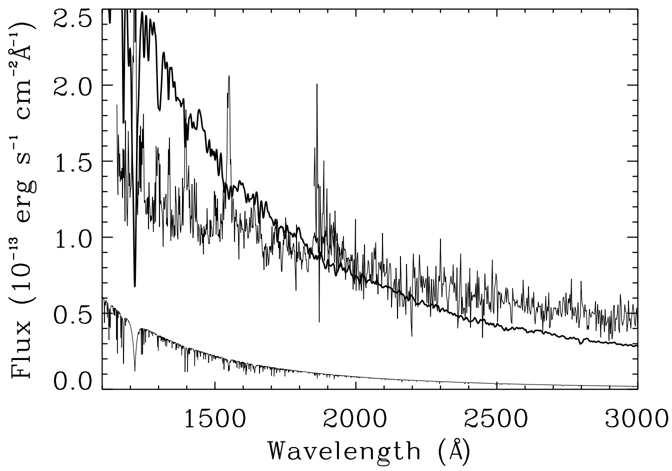

Fig. 4.—Fit of synthetic spectrum to intermediate-state *IUE* spectra of MV Lyr. The light line is the *IUE* spectrum; the heavy line is the synthetic spectrum. The synthetic spectrum includes a standard model accretion disk with a mass transfer rate of $1.0\times10^{-9}\ M_\odot\ {\rm yr}^{-1}$. The synthetic spectrum was convolved with a Gaussian 5 Å FWHM broadening function to match the *IUE* spectral resolution. The low-state synthetic spectrum from Fig. 1 (*lower spectrum*) is shown for comparison. [*See the electronic edition of the Journal for a color version of this figure.*]

We have investigated both options. The first permits a good fit to the *IUE* spectra, but the models are slightly inferior to the second-option models. The second option truncates the accretion disk at an inner radius larger than the WD radius (Long et al. 1994) and preserves the standard model $T(R)$ functional dependence on R. Since the distance to MV Lyr is a fixed quantity, as the truncation radius of the accretion disk is increased, producing an initial reduction in flux from the model and a resulting discrepancy with observed spectra, a compensating increase in the adopted mass transfer rate is necessary to restore agreement with the observed spectra. We started with the mass transfer rate of Figure 4, then incrementally increased the truncation radius and made compensating increases in the mass transfer rate. The quality of the successive fits improved but remained perceptibly discrepant (too blue) even up to a limiting truncation radius of $r_b/r_{\rm wd}=18$. At this truncation radius, 50% of the tidal cutoff radius, the necessary mass transfer rate becomes $1.0\times10^{-8}\ M_\odot\ {\rm yr}^{-1}$, close to the one used in L99, and 1 dex larger than the value given by Hameury et al. (1988) at the long-period boundary of the period gap. We conclude that a standard model $T(R)$ with a truncated accretion disk model produces a synthetic spectrum that is too blue and so does not fit the observed MV Lyr *IUE* spectra.

Our initial models maintained the WD $T_{\rm eff}$ of 47,000 K (H04). Sion (1995) has shown that mass transfer can cause compressional heating of WDs in CV systems by 10,000–20,000 K for mass transfer rates of order $1.0\times10^{-8}\ M_\odot\ {\rm yr}^{-1}$ or larger (also see Townsley & Bildsten 2002). We tested the model sensitivity to the WD $T_{\rm eff}$ by substituting a non-LTE, $T_{\rm eff}=52{,}000$ K, $\log g=8.25$ WD synthetic spectrum for the 47,000 K synthetic spectrum. The change in the system synthetic spectrum, for the wavelength range 1100–3000 Å, was almost undetectable at 3000 Å. In view of our much smaller mass transfer rate than those studied by Sion, we did not test larger $T_{\rm eff}$ values, and we do not consider this topic further.

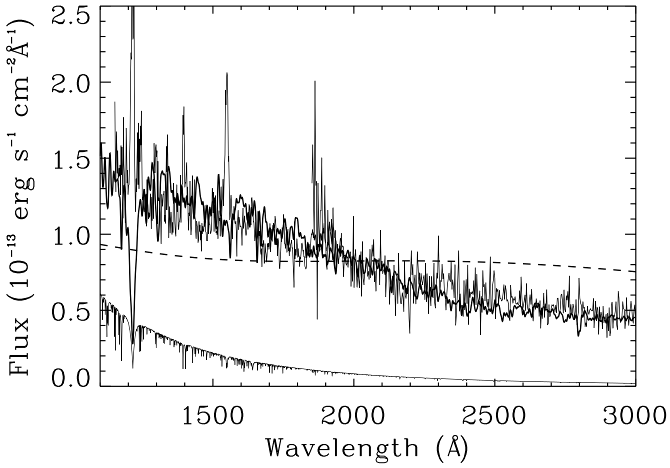

FIG. 5.—Same as Fig. 4, but with an accretion disk truncated at $r = 1.7r_{\rm wd}$, a $T(R)$ corresponding to a mass transfer rate of 6.0×10^{-10} $M_\odot$ yr^{-1}, and an isothermal 9500 K accretion disk beyond $r = 11.5r_{\rm wd}$. The dashed line represents a corresponding blackbody model. The light line is the *IUE* spectrum, and the heavy line is the synthetic spectrum. The low-state synthetic spectrum from Fig. 1 (*lower spectrum*) is shown for comparison. [*See the electronic edition of the Journal for a color version of this figure.*]

Our extensive experiments ultimately led us to a best-fitting model with a mass transfer rate of 6.0×10^{-10} $M_\odot$ yr^{-1}, a truncation radius of $r_b = 1.7r_{\rm wd}$, and with $T(R)$, which initially follows the standard model, set to 9500 K for radii larger than $11.5r_{\rm wd}$. The $T_{\rm eff}$ of the innermost annulus, including the correction for irradiation by the WD, is 30,195 K. Figure 5 shows the fit of this solution to the *IUE* data. The mean residual of the fit to the 877 points between 1150 and 3000 Å was 0.013, and the mean absolute residual was 0.158. These residuals apply to the scaled spectra. The synthetic spectrum is too blue. The dashed line represents a corresponding blackbody model in which all source synthetic spectra have been replaced by blackbody spectra of the same $T_{\rm eff}$. The blackbody model is not blue enough.

Křiž & Hubeny (1986, their Fig. 2) provide optical thickness as a function of wavelength for two TLUSTY-based accretion disk models. A rough interpolation indicates that our models likely are optically thick. If the accretion disk remains nearly Keplerian, our Figure 5 model, for equal bolometric luminosity, would correspond to a standard model of mass transfer rate higher than 6.0×10^{-10} $M_\odot$ yr^{-1}, and likely near 1.0×10^{-9} $M_\odot$ yr^{-1}.

We have not attempted to calculate irradiated models of the individual accretion disk annuli, a possible option in TLUSTY. Because of the disk truncation, no boundary layer has been included in the synthetic spectrum.

5. PREDICTED CHANGE IN *V* MAGNITUDE BETWEEN THE LOW AND INTERMEDIATE STATES

The AAVSO light curve shown in H04, and the Roboscope curve shown in Honeycutt & Kafka (2004), covering 1990–2004, reveals that MV Lyr exhibits high states lasting for 2–6 months, followed by low states lasting for similar lengths of time. Typical high-state *V* values are 12.2–12.8, while low-state *V* values are in the range 16–18. Intermediate-state magnitudes show considerable variation and are in the *V* range 13–15. Earlier *B* and *V* light curves (Rosino et al. 1993) cover the interval 1968–1991 and show that MV Lyr was in an extended low state from 1979 to 1989, with occasional transitions to intermediate states followed by returns to the low state.

Rosino et al. (1993) tabulate $B = 14.6$ on 1979 October 17, $B = 13.9$ on 1979 November 20, and $B = 17.6$ (a low state) on 1980 April 11. Since a typical $B - V$ value for MV Lyr is -0.25 (Rosino et al.), we estimate $V = 13.6$ at the time of the *IUE* intermediate-state observations (1979 December 2), roughly a magnitude below typical high-state values, and at the end of the intermediate state. We calculate a *B*-magnitude change of $\Delta B = 3.7$ mag from low state to intermediate state, with ΔV approximately the same. The Honeycutt & Kafka (2004) MV Lyr light-curve plot gives a typical intermediate state $-$ low state ΔV of 4.0.

We have calculated an extension of the Figure 5 model to 10,000 Å and have convolved the spectrum with the transmission profile of the *V* filter (Matthews & Sandage 1963). The normalized integral of this product tabulation is a measure of the theoretical *V* magnitude. This, together with a corresponding calculation with the low-state spectrum, extended to 10,000 Å, permits determination of the theoretical *V* magnitude change between the low and intermediate states. The Figure 5 model produces $\Delta V = 4.91$, compared with the observed 3.7 mag change in *B* (and *V*) between 1979 November 20 and 1980 April 11 (Rosino et al. 1993). We have calculated several models that fit the *IUE* spectra well, using elevated $T_{\rm eff}$ values in the outer part of the accretion disk, and all of them produce a ΔV that is at least 1 mag too large. If there is a bright spot in the intermediate-state system, the discrepancy is only made worse by adding a model of it to our calculated system model. This impasse indicates that a different approach is needed, and the blackbody plot in Figure 5 suggests that the difficulty is associated with the annulus synthetic spectra.

6. A LIMITING INTERMEDIATE-STATE MODEL

All of our models assume an outer boundary coincident with the tidal cutoff radius. Terminating the outer accretion disk boundary at a smaller value has the prospective advantage of reducing the flux at 5500 Å while having a minor effect at 3000 Å. We have followed this option to a limiting model: an isothermal 14,000 K accretion disk terminated at $r = 20r_{\rm wd}$. This termination radius produces a flux level that matches the observed spectrum, given the distance to MV Lyr. We have preserved a truncation radius at $r = 1.7r_{\rm wd}$, although the flux contribution from the innermost annuli is small. The calculated ΔV for this model, low to intermediate state, is 4.06, in good agreement with the Honeycutt & Kafka (2004) amplitude but larger than the Rosino et al. (1993) amplitude. Figure 6 shows the fit of this model to the *IUE* spectrum. The required flux level determines the accretion disk radius. The radiation peak at 1300 Å marks the same peak of the 14,000 K source synthetic spectrum of an annulus model. The fact that the limiting model synthetic spectrum is too blue is a property of the Balmer continuum region of the source synthetic spectrum, beyond the direct control of BINSYN. The blackbody plot of Figure 5 suggests that if formation of the continuum takes place under conditions that reduce the Balmer jump and slope of the Balmer continuum, then the Figure 6 model might fit the *IUE* spectra closely. Reducing the $T_{\rm eff}$ of the isothermal accretion disk to make it less blue requires an increase in the accretion disk radius to provide the necessary flux. This increases the *V* amplitude, producing a disagreement with observation. Our limiting model represents the best fit to the full array of observational data.

7. FIT TO THE HIGH-STATE *HST* SPECTRUM

As part of an *HST* snapshot program, we obtained a 730 s exposure of MV Lyr on 2003 June 24, when it was in a peak high state of $V \sim 12.5$. The Space Telescope Imaging Spectrograph (STIS) was used with grating G140L, giving a resolution near

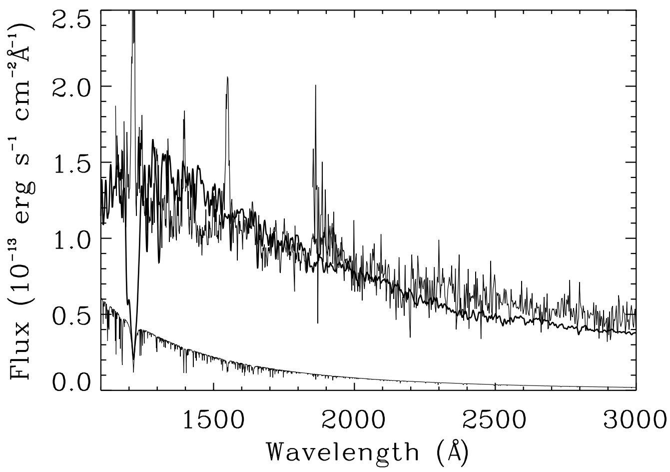

FIG. 6.—Same as Fig. 5, but with an isothermal 14,000 K accretion disk extending from an inner truncation radius at $r = 1.7r_{\rm wd}$ to $r = 20.0r_{\rm wd}$. The light line is the *IUE* spectrum, and the heavy line is the synthetic spectrum. The low-state synthetic spectrum from Fig. 1 (*lower spectrum*) is shown for comparison. [*See the electronic edition of the Journal for a color version of this figure.*]

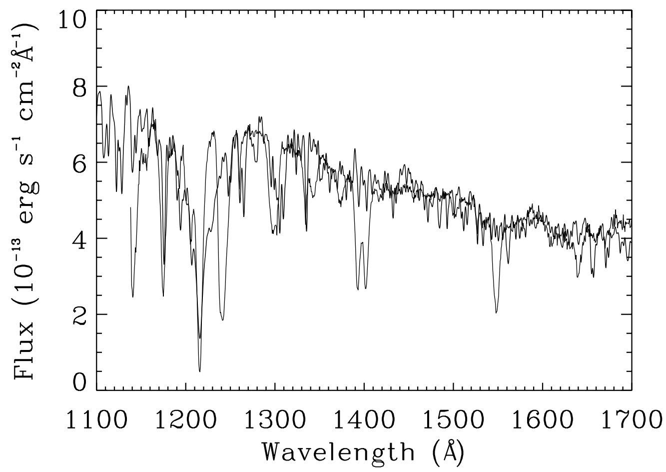

FIG. 7.—Fit of a standard model accretion disk with a mass transfer rate of 3.0×10^{-9} $M_\odot$ yr^{-1}, truncated at an inner radius of $1.7r_{\rm wd}$ and with annuli $T_{\rm eff}$ values set to 12,000 K beyond $r/r_{\rm wd} = 14.0$ (*heavy line*), to an *HST* high-state spectrum of MV Lyr (*light line*). The synthetic spectrum has been convolved with a Gaussian 1.2 Å FWHM broadening function. Line identifications are in subsequent figures. [*See the electronic edition of the Journal for a color version of this figure.*]

1.2 Å. Data reduction used the latest release of CALSTIS (ver. 2.13b). This version takes into account the decaying sensitivity of the G140L grating. All the lines are in absorption (Fig. 7, discussed below), consistent with an optically thick disk.

We investigated whether a standard model synthetic spectrum, including the option of a truncated accretion disk, can fit the *HST* spectrum. We began with the L99 mass transfer rate of 1.1×10^{-8} $M_\odot$ yr^{-1} and no truncation and found that the predicted flux for this model is appreciably too large at all *HST* wavelengths. The same mass transfer rate and an accretion disk truncated at $r/r_{\rm wd} = 6.2$ leads to a synthetic spectrum that is too blue and a slightly too small flux level, and an accretion disk truncated at $r/r_{\rm wd} = 5.3$ produces a synthetic spectrum that is too blue and a slightly too large flux level. Successively smaller mass transfer rates and no disk truncation produced models with flux levels still too large but with a smaller mean residual. At each mass transfer rate it was possible to find a pair of truncation radii for which the corresponding synthetic spectra bracketed the *HST* spectrum, one with slightly too large flux values, the other too small; in each case, both bracketing spectra were too blue. In addition to the initial test, we tested mass transfer rates of 7.0×10^{-9}, 5.0×10^{-9}, 4.5×10^{-9}, 4.0×10^{-9}, and finally 3.0×10^{-9} $M_\odot$ yr^{-1}. In this latter case an accretion disk extending to the WD surface fits the *HST* spectrum well between 1150 and 1200 Å but is much too blue (too little flux) longward of 1200 Å. Smaller mass transfer rates produce synthetic spectra with too small flux at all *HST* wavelengths. We conclude that standard model synthetic spectra, with or without truncated accretion disks, do not fit the *HST* spectrum; they are too blue.

With the objective to flatten the theoretical spectral gradient, we selected the standard model with small errors at the short-wavelength extreme, mass transfer rate of 3.0×10^{-9} $M_\odot$ yr^{-1}, and modified the $T(R)$ relation to an isothermal outer region with elevated temperature. We proceeded by initially selecting an accretion disk annulus at a large radius and setting the $T_{\rm eff}$ values of all annuli of larger radius to the $T_{\rm eff}$ of the selected annulus. The resulting synthetic spectrum provided an improved fit to the *HST* spectrum. We continued, gradually moving to a smaller crossover annulus and consequently higher $T_{\rm eff}$ value, until we reached a crossover annulus of $r/r_{\rm wd} = 14.0$ and annuli $T_{\rm eff} = 12{,}000$ K at larger radii. At smaller radii the annulus $T_{\rm eff}$ values continued to follow a standard model for a mass transfer rate of 3.0×10^{-9} $M_\odot$ yr^{-1}. The spectral gradient now was about correct but the overall flux level had become somewhat too large, and so we reduced the flux level by truncating the accretion disk. Because of the high $T_{\rm eff}$ value at the truncation radius, the color of the synthetic spectrum is mildly sensitive to the truncation radius value. We found an optimum fit with a truncation radius of $r/r_{\rm wd} = 1.7$ and a $T_{\rm eff}$ there of 43,404 K. It is likely that a slightly modified mass transfer rate, together with slightly changed truncation radius and crossover radius and outer annulus $T_{\rm eff}$ value, would fit the *HST* spectrum equally well. For that reason, we do not attribute special significance to the fact that the truncation radius found here is the same as the truncation radius for the intermediate state. The large differences between the *HST* spectrum and the synthetic spectrum absorption lines lead to larger mean and mean absolute residuals than for the intermediate and low states. The mean residual of the fit to the 970 points between 1150 and 1715 Å was -0.44, and the mean absolute residual was 0.71. These residuals apply to the scaled spectra.

Figures 7–10 show the fit to the *HST* spectrum of a synthetic spectrum with our optimum high-state parameters. Although the continuum is a reasonable fit, individual line fits show appreciable discrepancies, especially for the high-excitation lines of N v, Si iv, C iv, and He ii. Since all of our synthetic spectra assume solar composition, the discrepancies could arise from (1) abundance differences from solar composition or (2) excitation differences between the formation regions for the absorption lines and the continuum.

The observed absorption lines show a slight blueshift corresponding to a velocity of about -200 km s^{-1}. This effect is apparent in the detail plots, Figure 8 (C iii), Figure 9 (C ii, Si iv), and Figure 10 (C iv, He ii). Schneider et al. (1981) and Skillman et al. (1995) separately determine a system radial velocity of MV Lyr of $\gamma \simeq -35$ km s^{-1} from optical wavelength spectra. The velocity difference (of 165 km s^{-1}) is a clear indication that the absorption lines are formed in a wind. Since MV Lyr is viewed nearly pole-on, this means the wind has a low velocity. This interpretation is consistent with the observed line broadenings as listed in Table 2, e.g., the Si iv doublet near 1400 Å.

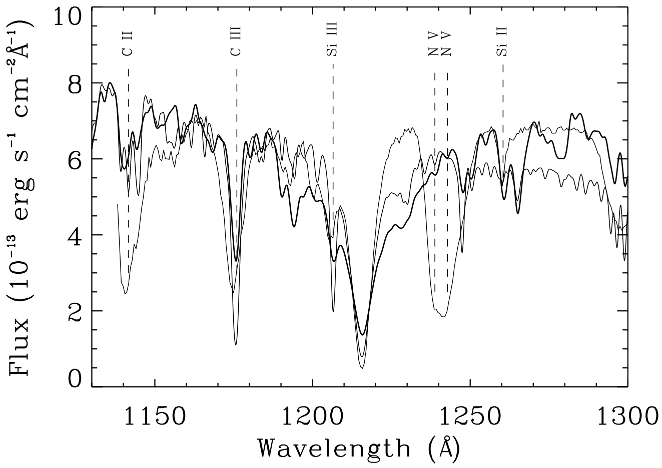

Fig. 8.—Detail of Fig. 7. The overplotted spectrum of intermediate thickness is a synthetic spectrum of a single annulus with a $T_{\rm eff}$ of 31,564 K, convolved with a Gaussian 1.2 Å FWHM broadening function. Note the much closer fit to the observed Lyα (*light line*) than provided by the system synthetic spectrum (*heavy line*). The annulus synthetic spectrum was divided by 6.5×10^8 before overplotting, to place the synthetic spectrum over the observed spectrum. [*See the electronic edition of the Journal for a color version of this figure.*]

Figure 8 shows the vicinity of Lyα. Note the much better fit of the overplotted annulus synthetic spectrum ($T_{\rm eff} = 31{,}564$ K) to the observed Lyα line than is true for the system synthetic spectrum, whose mean $T_{\rm eff}$ is appreciably lower. This indicates that the absorption lines are formed in a higher temperature environment (i.e., corona or wind) than is true for the continuum. Figure 9 shows the Si IV doublet near 1400 Å; it is too weak in the system synthetic spectrum, and equivalent widths for the overplotted annulus synthetic spectrum ($T_{\rm eff} = 31{,}564$ K) are again a better fit.

The C IV doublet (Fig. 10) in the system synthetic spectrum is also much too weak. The doublet is stronger in both of the overplotted annulus synthetic spectra ($T_{\rm eff} = 31{,}564$ and 38,076 K),

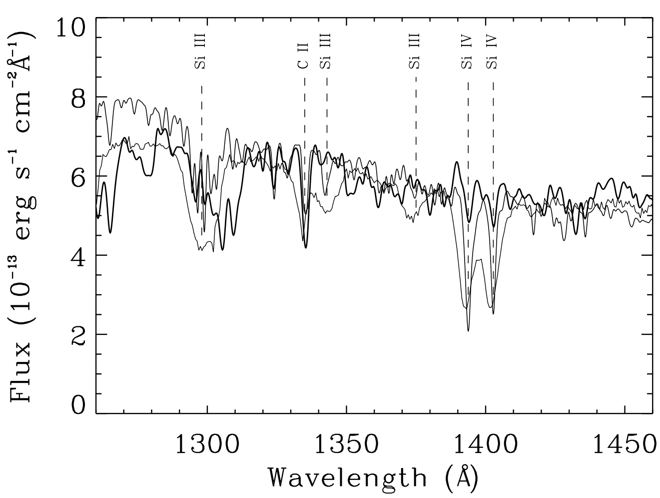

Fig. 9.—Same as Fig. 8, but for a different spectral region. The C II and Si III labels mark groups of transitions. Note that the Si IV equivalent widths in the overplotted annulus spectrum (31,564 K; *intermediate-thickness line*) are much greater than for the system synthetic spectrum (*heavy line*), indicating that the *HST* spectral lines (*light line*) are formed in a higher temperature environment than for the system synthetic spectrum. Note also that the observed Si IV lines are broadened, as well as displaced to shorter wavelengths. The annulus synthetic spectrum was divided by 4.7×10^8 before overplotting, to place the synthetic spectrum over the observed spectrum. [*See the electronic edition of the Journal for a color version of this figure.*]

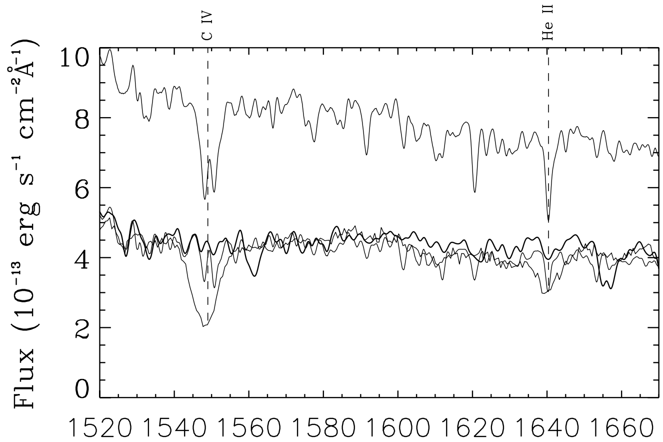

Fig. 10.—Same as Fig. 8, but for a different spectral region. Note that the equivalent widths of the C IV doublet and the He II line are appreciably greater in the overplotted annulus spectrum (31,564 K; *intermediate-thickness line*) than in the system synthetic spectrum (*heavy line*). The upper spectrum represents a 38,076 K annulus, shown for comparison, and with the same normalizing factor as the 31,564 K annulus. The annulus spectra were divided by 3.9×10^8 before overplotting, to place the 31,546 K synthetic spectrum over the observed spectrum. When scaled to fit the observed spectrum, the 38,076 K spectrum is fairly similar to the 31,546 K spectrum. Note that the C IV doublet is resolved in both annulus spectra and in the system synthetic spectrum. All three of these spectra have been convolved with a 1.2 Å Gaussian broadening function. [*See the electronic edition of the Journal for a color version of this figure.*]

but not by enough when scaled to fit the observed profile. The C II line complex (Fig. 9) is slightly too weak in the overplotted annulus spectrum, while the equivalent width of the system synthetic spectrum appears comparable to the observed value. The C III line complex, the overplotted annulus synthetic spectrum in Figure 8, appears to have an equivalent width approximately matching the observed value, while the system synthetic spectrum is too weak. The varying strengths of C lines in different ionization stages and the observed (large) strength of N V (Fig. 8) may be due to composition effects, but we cannot exclude the possibility that it is an excitation effect. Large N V/C IV ratios have been seen in several CV systems (Gänsicke et al. 2003) and are likely related to evolutionary effects. Note that H04 determine an overall metal

TABLE 2

Prominent Absorption and Emission Lines, FWHM Values

Ion	Nominal λ (Å)	*HST*	*IUE*	Low	Intermediate	High
C II	1141	10.5	...	0.5	5.8	4.4
C III	1175	6.3	1.4	2.6	2.6	3.2
N V	1241	11.5	1.2	2.6	1.0	1.8
Si II	1260	2.4	1.2	0.3	8.0	3.9
Si III	1299	12.3	2.0	2.2	1.7	4.8
C II	1334	3.0	7.5[a,b]	1.0	2.8	2.7
Si III	1342	9.9	...	1.0	2.7	3.1
	1374	8.6	1.5	1.6	1.3	1.6
Si IV	1393	6.4	7.0[a,b]	1.8	2.0	3.0
	1402	7.4	...	1.7	2.0	3.0
Si III	1501	6.6	7.0[a]	0.8	2.1	2.4
C IV	1549	7.9	10.8[a]	4.5	3.2	5.1
He II	1640	6.6	7.0[a]	3.4	3.0	3.4

Notes.—The *IUE* column refers to the intermediate-state spectrum, SWP07296. The columns designated as "low," "intermediate," and "high" refer to the system synthetic spectra corresponding to Figs. 1, 5, and 7, respectively.

[a] Emission line.

[b] This entry is the FWHM sum with the ion on the following line.

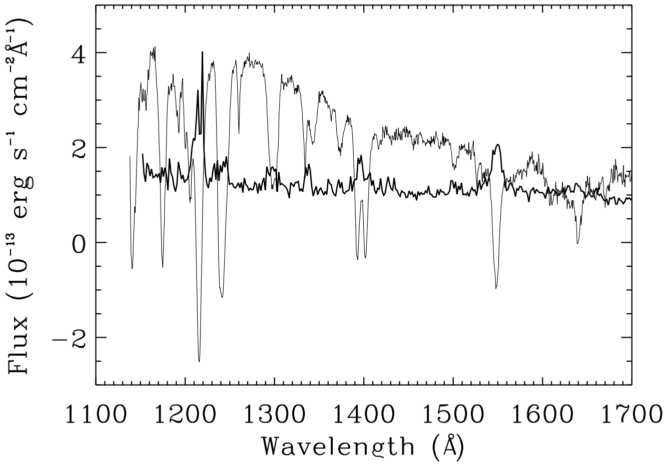

FIG. 11.—Comparison of the high-state *HST* spectrum (*upper spectrum*) and the intermediate-state *IUE* spectrum (*lower spectrum*) of MV Lyr. The high-state spectrum has been displaced downward by 3.0 flux units (ordinate scale) to superpose the C IV complex at 1540 Å. This plot demonstrates that the strong emission lines in the *IUE* spectrum become strong absorption lines in the *HST* spectrum, at (as well as can be determined) the same wavelengths and with similar broadening. A wavelength displacement as large as that between the *HST* spectrum and the synthetic spectrum in Fig. 9 would be detectable. Both sets of lines appear to be produced in a low-velocity wind.

composition for the MV Lyr WD of $Z = 0.3\ Z_\odot$, but detailed elemental abundances, relative to solar values, of C $= 0.5$, N $= 0.5$, and Si $= 0.2$. (Since strong excitation effects are clearly present, there is no conflict between our assumed solar abundance for the present analysis and the WD composition determination in H04.)

It is of interest to compare the emission-line spectrum of the intermediate state and the absorption-line spectrum of the high state (Fig. 11). Note that emission lines in the intermediate state match corresponding absorption lines in the high state. As well as can be judged, the relative strengths of the various resonance emission lines are similar to the relative strengths of the same absorption lines. The *HST* spectrum in Figure 11 has been displaced downward to superpose the C IV complex. The two broadened spectra fit accurately at the superposed line boundaries; if there were a radial velocity difference between the emission-line spectrum and the absorption-line spectrum as large as the displacement of the emission-line spectrum (e.g., Fig. 9) from the synthetic spectrum, that difference would be detectable. Comparable fits result when other spectral regions are superposed, although the low signal level of the *IUE* spectrum produces some ambiguity. It is of particular interest that the intermediate-state spectrum is flatter than the high-state spectrum. The two sets of lines in the intermediate and high states appear to be produced in a wind with a similar velocity structure in the two states.

8. CHANGE IN SYSTEM LUMINOSITY, LOW STATE TO HIGH STATE

The calculated *V* light change for our optimum model (Fig. 7) from low to high state, following the procedure of § 5, is 5.91 mag. The observed values are AAVSO, 6.0, and Honeycutt & Kafka (2004), 5.25, bracketing our calculated value. The *HST* observations provide a separate test. We used the STIS CCD acquisition image of MV Lyr to determine the magnitude at the time of the *HST* FUV observations to be 12.4 in the F28x50LP filter, corresponding to a monochromatic flux (but integrated over an extended spectral region) of $(2.205 \pm 0.05) \times 10^{-14}$ ergs cm^{-2} s^{-1} Å^{-1} at 7228.5 Å. The filter has a lower transmission limit at 5400 Å, a peak response at 6000 Å, and a gradual dropoff with half-peak response at 8300 Å and an upper transmission cutoff at 10,000 Å. The high-state model synthetic spectrum, when multiplied by this filter transmission and integrated, produces a calculated equivalent monochromatic 7228.5 Å flux, at the Earth for the 505 pc (H04) distance to MV Lyr, of 2.91×10^{-14} ergs cm^{-2} s^{-1} Å^{-1}, in approximate agreement with the observed value.

9. DISCUSSION

The significant result from our low-state study is that, to within observational error, the system spectrum can be represented by a combination of a WD spectrum and an irradiated, $T_{\rm eff,\,pole} = 2600$ K secondary component. There is no observational evidence for accretion disk emission in the MV Lyr low state. Our newly calculated contribution of the secondary star is an interpolation among NextGen models and includes allowance for irradiation of the secondary by the WD. Both L99 and HL02 model the low state of MV Lyr with a truncated accretion disk that retains most of its mass from the high state and emits radiation at a level consistent with residual viscosity. Our results limit possible low-state accretion disk emission to values well below those predicted by both L99 and HL02. Honeycutt et al. (1994) discuss the occasional sudden drops in luminosity of V974 Aql and show that the drops can be explained within the accretion disk limit cycle theory in terms of back and forth propagation of cooling and heating transition fronts. As with L99 and HL02, Honeycutt et al. (1994) find that the accretion disk undergoes little net mass loss while mass transfer from the secondary is turned off.

HL02 discuss slow passage of an accretion disk system from an initial stable state through the instability region and show that outside-in outbursts would occur but are unobserved. The only solution to the VY Sculptoris phenomenon that they visualize, to meet the constraint imposed by the case of TT Ari (Gänsicke et al. 1999), is a magnetic field sufficiently large ($B \gtrsim 6$ MG) to truncate the residual low-state accretion disk at a radius large enough to suppress accretion disk formation. However, as HL02 note, if a magnetic field is present, then circular polarization should also be present. Robinson et al. (1981) chronicle that repeated attempts to measure the circular polarization in MV Lyr always found a value of less than 0.13%. Robinson et al. also note that if there is a magnetic field present that is strong enough to disrupt the accretion disk, Zeeman-splitting of absorption lines should be detected; it is not. Thus, there is no evidence for a strong magnetic field associated with the MV Lyr WD.

Both the intermediate-state *IUE* spectra and the high-state *HST* spectra are inconsistent with our calculated standard models, having flatter flux profiles. Our subsequent thin-disk simulations, using TLUSTY annulus models, differ from the standard model by assuming a flatter $T(R)$ profile; they are able to produce fairly good fits to the observed continua. Confirmation that the TLUSTY annuli represent a thin-disk model is provided by the output data for an annulus at $r/r_{\rm wd} = 18.5$ and for a mass transfer rate of $4.0 \times 10^{-9}\ M_\odot$ yr^{-1}, close to the value of our high-state model. For this annulus, whose radius is 1.45×10^{10} cm, a Rosseland optical depth of 0.81 is located at $z = 1.94 \times 10^9$ cm, 1 dex smaller than the radius. A Rosseland optical depth of 0.001 occurs at $z = 1.98 \times 10^9$ cm, indicating line formation in a thin photosphere.

Smak (1994) has discussed peculiar (i.e., non–standard model), $T(R)$ distributions. The departures from the standard model in the systems he cites (e.g., Rutten et al. 1992) are in the direction of a too flat $T(R)$ profile, as we find for MV Lyr. Smak argues that the departures for systems with $i > 75°$ result from the assumption of a flat accretion disk. That explanation is not applicable to MV Lyr because of its low inclination. Smak suggests that for low-i cases, heating of the outer part of the accretion disk by the stream collision could be the explanation. Buat-Ménard et al. (2001) discuss the effect of stream impact heating and tidal effects. As our high-state model indicates, if stream impact heating is the physical cause of anomalous heating in the outer accretion disk region, the heating effects extend over an appreciable fraction of the accretion disk radius. This effect differs from a bright spot, for which the radial extent amounts to a few percent of the component separation (see Warner 1995, § 2.6.5). We stress the importance of the low orbital inclination in MV Lyr and the consequential absence of eclipses. All of the systems cited by Smak were shown to have peculiar $T(R)$ distributions by application of the MEM technique (Horne 1993) and so were restricted to systems showing eclipses. The spectrum synthesis method used in this paper represents an alternative and independent technique that is applicable to both eclipsing and noneclipsing systems.

The presence of high-excitation absorption lines in the MV Lyr system imply their formation in a high-temperature region above (both faces of) the accretion disk, possibly similar to a chromosphere or corona. Accretion disk coronae are considered in Meyer & Meyer-Hofmeister (1989, 1994), Liu et al. (1997), and Hameury et al. (2000). We have presented evidence for formation of both the intermediate-state emission lines and the high-state absorption lines in a wind, apparently coextensive with the high-temperature region. It would be of interest to search for a P Cygni profile, possibly in the infrared. We thank the referee for this suggestion. Drew (1997) summarizes known properties of winds from CVs. Proga et al. (1998) discuss a model of radiation-driven winds from accretion disks, and Pereya et al. (2004) discuss the stability of line-driven winds. Table 2 lists the FWHM wavelength ranges for the principal absorption lines in the *HST* spectrum. In most cases, several transitions contribute to a given line. The low MV Lyr i value nominally would imply narrow disk lines, distinctly different from the observations. The observed broadening is consistent with lines of sight that traverse a range of radial velocities before reaching an optical depth of 1.0. The 200 km s^{-1} blueshift of the absorption lines is smaller than typically found for winds from accretion disks.

Our TLUSTY annuli models are in LTE and apply default values for the internal parameters, leading to a negative temperature gradient perpendicular to the surface of the annulus. Line formation in a vertically extended wind violates our model assumption of hydrostatic equilibrium; addition of a wind model (Long & Knigge 2002) might provide improved representation of the MV Lyr spectral data. Froning et al. (2002) combined TLUSTY disk models with a representation of a biconical wind in a study of SS Cyg.

We speculate that continuum formation takes place under conditions different from the assumptions of our annulus models, and that difference may explain our failure to achieve an accurate continuum fit, especially in the intermediate state. Hubeny (1989a, 1989b) discusses conditions for hot upper layers of accretion disk annuli to exist. He shows that the z-direction profile of viscosity strongly affects the formation of these regions. Hubeny & Hubeny (1998) discuss the treatment of viscosity as implemented in TLUSTY, in particular the steps taken to prevent a high-temperature z-direction anomaly. The authors also emphasize the importance of non-LTE effects. It is widely believed that the physical cause of accretion disk viscosity is the magnetorotational instability (Balbus & Hawley 1991). Balbus (2002) discusses issues in the implementation of the instability in accretion disk models. The magnetohydrodynamic simulations of Stone et al. (1996) find an increase in viscosity toward the accretion disk surface, leading to increased z-direction heating.

The flatter spectral profile of the intermediate-state *IUE* spectrum, as compared to the *HST* high-state spectrum (Fig. 11), is of particular interest. The isothermal accretion disk extending only half-way to the tidal cutoff radius in the intermediate state has the attractive feature that it provides a ready explanation for emission lines (the line emission region is seen extending beyond the edge of the accretion disk), while the same lines are seen in absorption in the high state (the accretion disk now extends to the tidal cutoff radius). This scenario indirectly supports the absence of an accretion disk in the low state, again in disagreement with L99 and HL02. An explanation of the flat $T(R)$ profile, both intermediate and high, must differ from the case of DW UMa (Knigge et al. 2000; Araujo-Betancor et al. 2003), also a VY Sculptoris star. In DW UMa there is also a flat $T(R)$ profile, but it is explained by self-occultation by a puffed-up outer accretion disk rim and an orbital inclination large enough to produce eclipses of the WD.

10. SUMMARY

1. Given the excellent fit of a system synthetic spectrum to *FUSE*, *IUE*, and optical low-state spectra (H04), any accretion disk that may be present in the low state must have a $T_{\rm eff}$ value less than 2500 K. This result agrees with a study of the CV system TT Ari (Gänsicke et al. 1999). A comparison of our results (Fig. 3) with two models (L99 and HL02) of the VY Sculptoris phenomenon demonstrates a discrepancy with those models.

2. Using TLUSTY annulus models and corresponding synthetic spectra to simulate an intermediate state for which *IUE* spectra are available, we show that a standard model (see text) cannot produce a system synthetic spectrum that satisfactorily fits the *IUE* spectra. A rough fit is possible with a standard model with a mass transfer rate of 1.0×10^{-9} $M_\odot$ yr^{-1}, but the model synthetic spectrum is too blue. A fairly good fit is possible with a mass transfer rate of 6.0×10^{-10} $M_\odot$ yr^{-1}, a truncation radius of $r = 1.7r_{\rm wd}$, and $T(R) = 9500$ K beyond $r = 11.5r_{\rm wd}$. But this model produces a change in V magnitude between the low and intermediate states that is about 1 mag larger than the observational value. An isothermal 14,000 K accretion disk with a radius that is half of the tidal cutoff radius produces agreement with the V-magnitude change; this model is slightly bluer than the *IUE* spectra.

3. Study of a high state demonstrates that no combination of mass transfer rate and truncation radius can produce a standard model system synthetic spectrum whose continuum satisfactorily fits our recent *HST* spectrum. All synthetic spectra are too blue. A fairly good fit is possible for a mass transfer rate of 3.0×10^{-9} $M_\odot$ yr^{-1}, a truncation radius of $r = 1.7r_{\rm wd}$, and $T(R) =$ 12,000 K beyond $r = 14.0r_{\rm wd}$. This model produces a calculated system flux at 7228.5 Å that is in reasonable agreement with a measurement of *HST* optical flux.

4. The absorption lines in our MV Lyr *HST* spectrum show a range of excitations and corresponding temperatures that are higher than the nearly flat continuum would imply. This result is consistent with line formation in a large-z high-temperature region. Anomalous line strengths of C, N, Si, and He have a possible interpretation in terms of composition effects, but excitation effects cannot be disentangled.

5. The slight blueshift of the absorption lines (about −200 km s^{-1}), as compared with the system radial velocity of -35 km s^{-1}, indicates that the absorption lines are formed in a low-velocity wind, which is coextensive with the large-z high-temperature region. There is no apparent difference in velocity between the emission-line intermediate-state spectrum and the high-state absorption-line spectrum; the wind and high-temperature structures appear to be present in both the intermediate and high states.

6. The difference between the physical conditions under which the absorption and emission lines form in a wind and the physical conditions assumed by our hydrostatic equilibrium annulus models, used to calculate the synthetic spectra, may explain our difficulty in fitting the high-state and intermediate-state continua accurately. The same problem may explain the failure of our synthetic spectra to represent the high-excitation absorption lines in the high-state *HST* spectra.

We thank the anonymous referee for detailed comments that improved the presentation of this paper. A. P. L. and P. S. are grateful for partial support from NASA grant GO-9357 from the Space Telescope Science Institute and for *FUSE* grant NAG5-12203. P. S., K. S. L., and E. M. S. also acknowledge support for this work provided by NASA through grants GO-9357 and GO-9724 from the Space Telescope Science Institute, which is operated by AURA, Inc., under NASA contract NAS5-26555. B. T. G. was supported by a PPARC Advanced Fellowship.

REFERENCES

Andronov, N., Pinsonneault, M., & Sills, A. 2003, ApJ, 582, 358
Araujo-Beatncor, S., et al. 2003, ApJ, 583, 437
Armitage, P. J., & Livio, M. 1998, ApJ, 493, 898
Balbus, S. A. 2002, in ASP Conf. Ser. 261, The Physics of Cataclysmic Variables and Related Objects, ed. B. T. Gänsicke, K. Beuermann, & K. Reinsch (San Francisco: ASP), 356
Balbus, S. A., & Hawley, J. F. 1991, ApJ, 376, 214
Buat-Ménard, V., Hameury, J.-M., & Lasota, J.-P. 2001, A&A, 366, 612
Drew, J. E. 1997, in IAU Colloq. 163, Accretion Phenomena and Related Outflows, ed. D. T. Wickramasinghe, L. Ferrario, & G. V. Bicknell (ASP Conf. Ser. 121; San Francisco: ASP), 465
Frank, J., King, A., & Raine, D. 1992, Accretion Power in Astrophysics (2nd ed.; Cambridge: Cambridge Univ. Press)
Froning, C. S., Long, K. S., Drew, J. E., Knigge, C., Proga, D., & Mattei, J. A. 2002, in ASP Conf. Ser. 261, The Physics of Cataclysmic Variables and Related Objects, ed. B. T. Gänsicke, K. Beuermann, & K. Reinsch (San Francisco: ASP), 337
Gänsicke, B. T., Sion, E. M., Beuermann, K., Fabian, D., Cheng, F. H., & Krautter, J. 1999, A&A, 347, 178
Gänsicke, B. T., et al. 2003, ApJ, 594, 443
Hamada, T., & Salpeter, E. E. 1961, ApJ, 134, 683
Hameury, J.-M., King, A. R., Lasota, J.-P., & Ritter, H. 1988, MNRAS, 231, 535
Hameury, J.-M., & Lasota, J.-P. 2002, A&A, 394, 231 (HL02)
Hameury, J.-M., Lasota, J.-P., & Warner, B. 2000, A&A, 353, 244
Hauschildt, P. H., Allard, F., & Baron, E. 1999, ApJ, 512, 377
Hoard, D. W., Linnell, A. P., Szkody, P., Fried, R. E., Sion, E. M., Hubeny, I., & Wolfe, M. A. 2004, ApJ, 604, 346 (H04)
Honeycutt, R. K., Cannizzo, J. K., & Robertson, J. W. 1994, ApJ, 425, 835
Honeycutt, R. K., & Kafka, S. 2004, AJ, 128, 1279
Horne, K. 1993, in Accretion Disks in Compact Stellar Systems, ed. J. C. Wheeler (Singapore: World Scientific), 117
Hubeny, I. 1988, Comput. Phys. Commun., 52, 103
———. 1989a, in Theory of Accretion Disks, ed. F. Meyer, W. Duschl, J. Frank, & E. Meyer-Hofmeister (NATO ASI Ser. C, 290; Dordrecht: Kluwer), 445
———. 1989b, in Space Sci. Rev., 50, 117
Hubeny, I., & Hubeny, V. 1998, ApJ, 505, 558
Hubeny, I., & Lanz, T. 1995, ApJ, 439, 875
Hubeny, I., Stefl, S., & Harmanec, P. 1985, Bull. Astron. Inst. Czechoslovakia, 36, 214
King, A. R. 1988, QJRAS, 29, 1
King, A. R., & Cannizzo, J. K. 1998, ApJ, 499, 348
King, A. R., & Schenker, K. 2002, in ASP Conf. Ser. 261, The Physics of Cataclysmic Variables and Related Objects, ed. B. T. Gänsicke, K. Beuermann, & K. Reinsch (San Francisco: ASP), 233
Knigge, C., Long, K. S., Hoard, D. W., Szkody, P., & Dhillon, V. S. 2000, ApJ, 539, L49
Kříž, S., & Hubeny, I. 1986, Bull. Astron. Inst. Czechoslovakia, 37, 129
Lasota, J.-P. 2001, NewA Rev., 45, 449
Leach, R., Hessman, F. V., King, A. R., Stehle, R., & Mattei, J. 1999, MNRAS, 305, 225 (L99)
Linnell, A. P., Hoard, D. W., Szkody, P., & Fried, R. E. 2005, in ASP Conf. Ser., Astrophysics in the Far Ultraviolet: Five Years of Discovery with *FUSE*, ed. G. Sonneborn, W. Moos, & B.-G. Andersson (San Francisco: ASP), in press
Linnell, A. P., & Hubeny, I. 1996, ApJ, 471, 958
Liu, B. F., Meyer, F., & Meyer-Hofmeister, E. 1997, A&A, 328, 247
Livio, M., & Pringle, J. E. 1994, ApJ, 427, 956
Long, K. S., & Knigge, C. 2002, in ASP Conf. Ser. 261, The Physics of Cataclysmic Variables and Related Objects, ed. B. T. Gänsicke, K. Beuermann, & K. Reinsch (San Francisco: ASP), 327
Long, K. S., Wade, R. A., Blair, W. P., Davidsen, A. F., & Hubeny, I. 1994, ApJ, 426, 704
Matthews, T. A., & Sandage, A. R. 1963, ApJ, 138, 30
Meyer, F., & Meyer-Hofmeister, E. 1989, A&A, 221, 36
———. 1994, A&A, 288, 175
Orosz, J. A., & Wade, R. A. 2003, ApJ, 593, 1032
Patterson, J. 1984, ApJS, 54, 443
Pereya, N. A., Owocki, S. P., Hillier, D. J., & Turnshek, D. A. 2004, ApJ, 608, 454
Proga, D., Stone, J. M., & Drew, J. E. 1998, MNRAS, 295, 595
Ritter, H. 1988, A&A, 202, 93
Robinson, E. L., Barker, E. S., Cochran, A. L., Cochran, W. D., & Nather, R. E. 1981, ApJ, 251, 611
Rosino, L., Romano, G., & Marziani, P. 1993, PASP, 105, 51
Rutten, R. G. M., van Paradijs, J., & Tinbergen, J. 1992, A&A, 260, 213
Schenker, K., & King, A. R. 2002, in ASP Conf. Ser. 261, The Physics of Cataclysmic Variables and Related Objects, ed. B. T. Gänsicke, K. Beuermann, & K. Reinsch (San Francisco: ASP), 242
Schneider, D. P., Young, P., & Shectman, S. A. 1981, ApJ, 245, 644
Schreiber, M. R., Gänsicke, B. T., & Cannizzo, J. K. 2000, A&A, 362, 268
Shakura, N. I., & Sunyaev, R. A. 1973, A&A, 24, 337
Sion, E. M. 1995, ApJ, 438, 876
Skillman, D. R., Patterson, J., & Thorstensen, J. R. 1995, PASP, 107, 545
Smak, J. 1994, Acta Astron., 44, 265
Stone, J. M., Hawley, J. F., Gammie, C. F., & Balbus, S. A. 1996, ApJ, 463, 656
Szkody, P., & Downes, R. A. 1982, PASP, 94, 328
Townsley, D. M., & Bildsten, L. 2002, in ASP Conf. Ser. 261, The Physics of Cataclysmic Variables and Related Objects, ed. B. T. Gänsicke, K. Beuermann, & K. Reinsch (San Francisco: ASP), 31
Visniac, E. T., & Diamond, P. 1989, ApJ, 347, 435
———. 1992, ApJ, 398, 561
Warner, B. 1995, Cataclysmic Variable Stars (Cambridge: Cambridge Univ. Press)